Rich interfacial chemistry and properties of carbon-doped hexagonal boron nitride nanosheets revealed by electronic structure calculations

Wei Xie[1]†, Takahiro Tamura[1], Takashi Yanase[1], Taro Nagahama[1], Toshihiro Shimada[1]*

1. Division of Applied Chemistry, Faculty of Engineering, Hokkaido University

Kita 13 Nishi 8, Kita-ku, Sapporo 060-8628, Japan

*E-mail: shimadat@eng.hokudai.ac.jp

The effect of C doping to hexagonal boron nitride (h-BN) was examined by first principle calculations with the association of π-electron systems of organic molecules embedded in a two dimensional insulator. In mono-layered carbon doped structure, odd number doping of carbon atoms lead to a metallic properties with different work functions. A variety of electronic interactions was found in the interaction between two layers with odd number carbon substitution. Direct sp^3 covalent chemical bond is formed when C is replacing adjacent B and N in the different layers. Charge transfer complex between layers was found when the C is replacing next atoms, which results in narrow band gaps (e.g. 0.37eV). Direct bonding between C and B atoms was found when two C atoms in different layers are in distance.

†Present Address: Frontier Energy Research Division, Inamori Frontier Research Center, Kyushu University

1. Introduction

Graphite and hexagonal boron nitride (h-BN) have analogous crystal structures but exhibit much different electronic properties. Graphite is a metal with two unfilled bands and h-BN is a wide band gap (E_g = 4.5eV) semiconductor. We can expect that a wide variety of semiconductors with tunable band gaps will be synthesized by making their alloys (hexagonal $C_xB_yN_z$; h-CBN) with well-defined structures. A variation of h-CBN is gathering much attention recently as graphitic-C_3N_4 photocatalysts[1)], to which boron doping is also attempted[2)]. Considerable efforts are being made to synthesize monolayer h-CBN using chemical vapor deposition on metal surfaces from methane and borazine[3,4)] or sophisticated organic molecules[5)]. These progresses stimulate our curiosity about the bulk properties of carbon-doped h-BN. It should be noted that C-doped h-BN structures have resemblance with π-conjugated organic molecules and stacking of h-CBN has analogy with organic semiconductor crystals.

Recent theoretical works have revealed some of the interesting electronic structures of h-CBNs.[6-20)] Single carbon dopant in h-BN makes midgap trap states, dopants tend to aggregate, and substantial band dispersion is expected with multiple carbon doping. These are uplifting results for the development of new group of semiconductors that are light-weight and composed of naturally abundant elements. However, the theoretical analyses of this important class of materials have been limited only to the graphene-like monolayers of h-CBN.

Experimentally, however, distinct physical properties predicted by calculation have not been confirmed well, despite the long history of research on this class of material[21-25)]. The primary reason is that the physical properties, such as work function and band gaps, are very sensitive to the structural variation. Although it has been evaluated by computational studies for monolayer h-CBNs, interlayer interaction has not been studied well. The main purpose of this work is to clarify the electronic structures of double layer h-CBN. We briefly extend our previous work[20)] on uneven substitution (h-$C_xB_yN_z$ with $y \neq z$) and then examine the interlayer interaction of two layers. A part of this paper was presented in SSDM 2017 briefly without quantitative values of structural and electronic parameters,[26)] but this paper explains the simulation results quantitatively and in more detail.

2. Calculation methods

All the calculations in this work were carried out on the Quantum-Espresso[27] 5.1, which is based on density-functional theory (DFT), plane wave and pseudopotentials. VASP[28] 5.3 was also used in some cases and the results were identical within the accuracy. DFT was carried out with the exchange-correlation energy treated by the Perdew-Burke-Ernzerhof (PBE) functional based on the generalized gradient approximation (GGA).[29] Ultrasoft pseudopotentials[30] were used to describe the ionic cores, and the electron wave function was expanded in plane wave with the cut-off energy of 100 Ry for the geometry optimization and electronic structure calculations. The mono-layered hybrid structures of h-CBN were modeled by a 4 × 4 h-BN supercell with 32 atoms, and the double-layered hybrid structures of h-CBN were also modeled by doping carbon atoms to a 3 × 3 × 2 h-BN supercell with 36 atoms in a space group of P63/mmc. More than 10Å vacuum space as periodic boundary conditions along c-axis avoids interactions between layers in two neighboring cells. The atom positions were optimized until the forces on each ions converged in 0.0001 a.u. and the energy was converged in 1.0×10^{-6} eV. The band structure, density of states (DOS) and the electron localization function (ELF)[31,32] have been calculated by using the special k points of 9 × 9 × 1 (mono-layers) and 9 × 9 × 3 (double-layers) in the Brillouin zone of the supercell.[33] The comparison with previous results of established materials systems have been described in Ref. 20, which shows reasonable agreement.

3. Results and discussion

3.1 Unbalanced substitution in a monolayer

Single atom substitution of B or N by carbon atom gives half-filled flat midgap states as reported in Ref. 16. A balanced substitution of B and N by multiple carbon atoms makes intrinsic semiconductors. Here we calculated structures with odd-number substitution with multiple carbon atoms. Typical examples of odd number substitutions are shown in Fig. 1. Figures 1(a) and 1(b) are single atom substitution of B and N, respectively. Figures 1(c) and 1(d) show three atoms substitution of 3 B atoms by 3 C atoms and 3 N atoms by 3 C atoms, respectively. Figures 1(e) and 1(f) shows substitution of 1 B atoms and 2 N atoms by 3 C atoms, and 2 B atoms and 1 N atoms by 3 C atoms, respectively. The electronic band

structures of these hypothetical materials are shown in Fig. 2. Figures 2(a) - 2(f) corresponds to Fig. 1(a) - 1(f), respectively. The band structures in Fig. 2 are all metallic, as expected from the odd numbers of electrons in the unit cell. It should be noted that the Fermi levels indicated by horizontal broken lines are strongly dependent on which of B and N are replaced more. It means that the work function values of these materials are switchable in a wide range of 2 ~ 3 eV, which is an intriguing feature of them. It should also be noted that the band dispersion increases by increasing the number of C atoms. The small but finite band dispersion in Figs. 2(a) and 2(b) is different from the previously reported flat impurity bands of single dopant cases[15]. The discrepancy is due to the interaction between C atoms beyond the periodic boundary in the present calculation, of which supercell is smaller than previous calculations.

In order to see how the influence of carbon dopants laterally propagates, Two dimensional ELF (2D-ELF) were calculated for the further analysis. ELF is frequently used to visualize chemical bonds explicitly[31,32]. Figure 3 shows the ELF distributions of the monolayers shown in Fig. 1 in addition to pure h-BN (designated as “BN” in Fig. 3). In pure h-BN, the boron and nitrogen atoms have totally different distributions of electrons, *i.e.*, the red area (high density of electron pairs) gathered around the nitrogen atoms, while the blue area (low density of electron pairs) gathered around the boron atoms, which reflects the difference in the nuclear charge. In the structure (a), the electron density around the embedded carbon atom is intermediate between that around the boron atoms and nitrogen atoms. The opposite situation in the structure (b), in which a carbon atom substituted a nitrogen atom, a high electron density similar with nitrogen atoms is observed around the carbon atom. In the structures (c) and (d), the three carbon atoms are separately embedded in the h-BN system. The 2D-ELF distrubution around carbon atoms in (c) and (d) are very similar to those in (a) and (b), which means that the three carbon atoms have rather isolated electronic states. It is consistent with the band structures that show small dispersion of carbon-derived bands. The last two 2D-ELF, Figs. 3(e) and 3(f), correspond to the hybrid structures shown in Figs. 1(e) and 1(f), respectively. In Fig. 3(e), the electron pair distribution around the carbon structures show the totally different shape from the rest BN network which means that the embedded carbon structures formed a new π-conjugated electron system. Furthermore, the electron pair distribution around the B and

N adjacent to the carbon atoms are also modified. It corresponds to the band dispersion modified in LUMO-1 and HOMO band in Fig. 2(e). Similar feature can be observed in Fig. 3(f).

In the analysis above, the hybrid h-CBN systems with unbalanced substitution show the metallic nature with very different electron affinity or work function values. This result implies that a spontaneous electron transfer might occur by stacking differently doped h-CBN. In the next section we will examine it.

3.2 Interaction between layers in double layers

We examined the electronic structures of C-doped h-BN double layers. In the ordinary h-BN (P63/mmc), the atoms in each layer are overlapped along c-axis, and B and N atoms are stacked alternatingly. Figure 4 shows double-layered h-CBN structures studied in this work. They are shown after the structural optimization. Figure 4(a) shows the case of the nearest interlayer C-C distance, denoted as "2C-i" structure, in which two carbon atoms in total substitute a B atom in the upper layer and an N atom in the lower layer. The C atoms are stacked with the same position in the plane. Figures 4(b) and (c) depict the structures of "2C-ii" and "2C-iii", respectively. The difference among "2C-*n*" (*n* = i,ii,iii) is the distances between the carbon atoms. In 2C-ii and -iii, the C atom of the lower layer is shifted toward (1 -1 0) direction by one atom and two atoms, respectively.

The optimized structures of these cases of single atom substitution per layer are much different as observed in Fig. 4. In the "2C-i" case (Fig. 4(a)), in which carbon layer in the different layer is nearest, carbon atoms come together to the distance of h_2=1.67 Å. The bond lengths of nearest intra-layer distances of C-N and C-B in the top and the bottom layers are 1.47 Å and 1.56 Å, respectively. In the intermediate "2C-ii" case (Fig. 4(b)), the doped carbon in the top layer deviated from the layer by h_1=0.69Å toward the lower layer, while that in the bottom layer had not shifted significantly, resulting in interlayer distance at the shortest point to be h_2=2.71 Å. In "2C-iii" structure (Fig. 4(c)), the doping carbon in top layer have a significant deviation with the value of h_1=0.82Å deviated from the top layer while the carbon atom in bottom layer show no changes. Instead, a boron atom in the bottom layer has shifted toward the top layer by h_3=0.67 Å. This boron atom is just beneath the carbon atom in the top layer, while nitrogen atom is on directly beyond the carbon atom in

the bottom layer. It seems that this difference cause the apparent asymmetry of the behavior of the carbon atoms. The interlayer C-B distance of the shifted pair is 1.76 Å. Based on the structural information on "2C-i" and "2C-iii", we can conclude that they have direct chemical bonds between layers. The distance between interlayer C-C in "2C-i" (1.67Å) is shorter than that of interlayer C-B in "2C-iii" (1.76Å), suggesting that the C-C bond is more stable than C-B bonds.

We also calculated the structure with three doped carbon atoms per layer. "6C-i" (Fig.4(d)) has the carbon atoms of the top and the bottom layers are facing to each other, in a similar fashion with "2C-i". The shortest interlayer C-C distance in "6C-i" is 1.67 Å, which is the same value as that of "2C-i". The bond lengths of C-N and C-B in top and bottom layer are 1.47Å and 1.53Å in "6C-i" structure, respectively, which are similar to those of "2C-i". In "6C-ii" (Fig.4(e)) structure, the deviations of carbon from the layers have been more weakened than in "2C-ii". The displacement of carbon atoms from both layers is less than 0.1Å, which is slightly less than "2C-ii". The structure with three carbon atoms per layer corresponding to "2C-iii" was not calculated because of the limitation of the supercell.

The band gaps of all the structures are listed in Table 1, which came from the band structure calculation (shown in Fig. 5). In the structures "2C-i" and "6C-i" shown in Figs. 5 (a) and 5(b), respectively, the band gaps are great compared to other structures (3.75eV and 3.25eV, respectively). This result means that by stacking the two kinds of metallic layers (B-rich h-CBN layer and N-rich h-CBN layer), the free electrons will pair together. The band structures of "2C-ii" and "6C-ii are shown in Figs. 5 (c) and (d), respectively. The both of them show small band gaps with the value of 0.36eV and 0.61eV, respectively. The band gaps are much smaller than that of "2C-i" and "6C-i". Although the carbon content was increased from 2 to 6, the band gap of "6C-ii" increased from "2C-ii", which is different from the general tendency of monolayers or "2C-i" and "6C-i". Both of "2C-ii" and "6C-ii" are not metallic because neither of them have the energy levels crossing Fermi level. Figure 5(e) shows the bands structure of "2C-iii". The band gap is indirect; the HOMO-band top is located at Γ-point while LUMO-band bottom is located at K-point. The value of the band gap is 2.69 eV. This band gap is also smaller than that of "2C-i" (3.75eV), but larger than that of "2C-ii" (0.32eV). Interestingly, in the band structure of "2C-iii", the HOMO crosses the Fermi level, which means that structure "2C-iii" is metallic and unpaired electrons exist in

this structure. From the analysis so far, the resemblances of electronic structures of “2C-i” and “6C-i”, and “2C-ii” and “6C-ii” are apparent. Therefore, we will focus on the “2C-*n*” (*n* = i,ii,iii) structures in the following.

The wave function distributions of HOMO and LUMOs are shown in Fig. 6. Figures 6 (a) and (b) exhibit the HOMO and LUMO of “2C-i”, respectively. HOMO of “2C-i” is located on N atoms. LUMO is mainly located on the B atoms while a small part is located on C atoms. The HOMO and LUMO are mainly contributed from B and N atoms adjacent to the C atoms. It means that the C atoms change the electronic structure of neighboring B and N atoms, and make them more active than other B and N atoms which are far away. In the monolayers HOMO and LUMO are located on the C atoms, while in “2C-i” the contribution of C atoms is weak. This result can be explained by considering that the sp^3 carbon atoms formed by interlayer bonding in “2C-i” have more stable electronic structures. HOMO and LUMO of “6C-i” (not shown) have similar features as “2C-i”.

The HOMO and LUMO of “2C-ii” are shown in Figures 6(c) and (d), respectively. In “2C-ii”, the HOMO and LUMO are mainly allocated at the C atoms. Both of C atoms contribute to both of HOMO and LUMO, which means that the C atoms are active and they can be both electron donors and acceptors. This mixed contribution of C atoms to both of HOMO and LUMO seems important as the mechanism of narrowing band gaps with low carbon content. This point will be discussed later using the charge and ELF distributions. Finally, Figs.6 (e) and (f) shows the HOMO and LUMO of “2C-iii”. In this figure, HOMO is mainly distributed in the top layer, around the N atoms adjacent to the doped C atom. On the other hand, LUMO is distributed in the bottom layer, around the C atom and the N atom adjacent to the C atom and N atoms around the displaced B atom. In the top layer, the doped C atom neither contributes to the HOMO nor LUMO. Considering the displacement of the C atom of the top layer, this C atom might have sp^3 configuration, which has deep levels.

In order to directly show the modification of electronic structure and the distributions of electrons, especially interlayer electron transfer, ELF was calculated and the results are shown in the following figures. In “2C-i” shown in Fig. 7, a large ELF cloud can clearly be observed between two doped carbons along the C-C direction. It is the typical electron distributions in σ-bonds, which means that in this structure “2C-i” the carbon atoms exist as

sp^3 carbons. It is reasonably understood that the band gap of "2C-i" is great because sp^3 carbon have large energy gaps and do not contribute to narrow the band gap.

In the ELF figure of "2C-ii" shown in Fig 8, C atom a in the top layer (marked "a") has an electron cloud which is localized on the p_z-orbital (z is perpendicular to the layer), in addition to the three electron cloud along neighboring three N atoms. On the other hand, the C atom in the bottom layer (marked "a'"), there are no electrons located at the p_z-orbital. It suggests that one electron is transferred from "a'" in the bottom layer to "a" in the top layer. Indeed the electron counting indicates that 0.415 e^- are donated from the bottom layer to the top layer. In other words, "2C-ii" is a kind of charge-transfer (CT) complex. The narrow band gap is naturally explained because it is one of the important features of the CT complex [34].

Since the bandgap of "6C-ii" (0.61eV) is greater than that of "2C-ii" (0.36eV) but still much smaller than that of BN (4.53eV), the tunability of CT complex was examined by taking another example in "6C-ii". In "6C-ii", the shape of the electron distributions between C-C (Fig. 9) means that beside the σ bonds, C-C is also contributed from π-electron structures. The doped carbon atoms form two π-electron structures separately in different layers. From this ELF figure, it is hard to tell where the new electron pair is located and the direction of the electron transfer. In "6C-ii", the electrons around C atoms are delocalized. The new electron pair contributes to π-electron structures among the three carbons in the same layer. By the close analysis, it was found that the electron transfer was from the bottom layer to the top layer (N-rich layer to B-rich layer) and the amount was 0.32 e^- in this extended unit cell. This charge difference indicates that the spontaneous electron transfer behavior still exists in "6C-ii" structure, but it is weakened. It is consistent with the bandgap of "6C-ii" larger than "2C-ii". Doping multiple (odd numbered) C atoms tend to form more stable electronic structures in their own layers than isolated C atoms do.

In the ELF distribution of "2C-iii" shown in Fig.10, the existence of the electron cloud between the C atom and underneath B atom means that these two atoms directly bond together. Both of the C atom and the B atom exist with the stable sp^3 state. It is the reason of this C atom does not contribute to the HOMO or LUMO. The B atom, as a new electron donor, forms covalent bond with the C atom. However, the other C atom in the bottom layers (N-rich layer), an unpaired electron still located at the C atom, which makes the C

atom more active than the C atom in the top layer. This is the reason of the metallic features. The interlayer charge transfer exists in “2C-iii”, but the amount was 0.17 e^-, which is much smaller than those in type ii (*i.e.* “2C-ii” and “6C-ii”).

Finally, we examined the double-layered h-CBN with the even doping carbon number. The results are not shown as figures, but the distance of the two layers after optimization was 3.4 Å without any significant changes in vertical direction from pure double-layered h-BN. The doped carbon atoms also did not show a significant position shift. Based on the optimized structures, the two layers are independent. The band gap was 3.09eV. It is noticed that all the band dispersion curves are made of almost parallel two curves; it is due to the layered structure with very weak interaction.

Now we would like to comment on the comparison of the present results with the experiments. h-CBN can be synthesized by CVD or plasma CVD but the electronic structures are sensitive to the growth conditions[35-37]. We found that the electronic structures are very sensitive to the geometry of the doping (C numbers, arrangements, etc.). It can account for the difficulty to control the electronic structures of the materials. In the future, some methods will be found to synthesize h-CBN as designed in the atomic level, and then it will open a way to variety of physical properties of this group of materials. We hope the present work will stimulate further experiments on the electronic structure of h-CBN system as well as their applications. Once well-defined hexagonal B-C-N strucrtures can be synthesized, the applications will be photo catalysts using tunable bandgaps, catalysts using the partially localized electrons, and sensors with partial chemical bonding with adsorbed molecules. Various experimental methods are now under development [38-41] for the controlled synthesis.

4. Conclusions

The effect of C doping to hexagonal boron nitride (h-BN) was examined by first principle calculations with the association of π-electron systems of organic molecules embedded in a two dimensional insulator. In mono-layered carbon doped structure, odd number doping of carbon atoms lead to a metallic properties with different work functions. Variety of electronic interactions was found in the interaction between two layers with odd

number carbon substitution. Direct sp^3 covalent chemical bond is formed when C is replacing adjacent B and N in the different layers. Charge transfer complex between layers was found when the C is replacing next atoms, which results in narrow band gaps (e.g. 0.37eV). Direct bonding between C and B atoms was found when two C atoms in different layers are in distance. The tunability of the band gap and the workfunction of these materials will be very important for the application in electronics. It is desired to develop methods to control the stoichiometry and local structure of the materials because the electronic properties are sensitive to the local structures.

Acknowledgments

The present work has partly been supported by KAKENHI 17H0338007 and CREST-JST. The authors thank the Supercomputer Center, the Institute for Solid State Physics, The University of Tokyo for the use of the facilities.

References

1) X.C. Wang, K. Maeda, A. Thomas, K. Watanabe, G.Xin., J.M. Carlsson, K.Domen, and M. Antonietti, Nat. Mater. 5, 76 (2009).
2) S.C.Yang, Z.S.Li, and Z.G. Zou, Langmuir 26, 3894 (2010).
3) L. Ci, L. Song, C. Jin, D. Jariwala, D. Wu, Y. Lim A. Srivastava, Z.F. Wang, K. Storr, L. Balicas, F. Liu, and P.M. Ajayan, Nat. Mater. 9, 430 (2010).
4) C. Zhang, S. Zhao, C. Jin, A.L.Koh, Y. Zhou, W. Xu, Q. Li, Q. Xiong, H. Peng, and Z. Liu, Nat. Commun. 6:6519 (2015).
5) C. Sanchez-Sanchez, S. Bruller, H.Sachdev, K. Mullen, M. Krieg, H.F. Betinger, A. Nicolai,V. Meunier, L. Talirz, R. Fasel, and P. Ruffieux, ACS Nano 9, 9228 (2015).
6) M.S.C. Mazzoni, R.W. Nunes, S.Azevedo, and H.Chacham, Phys. Rev. B 73, 073108 (2006).
7) K. Yuge, Phys. Rev. B79, 144109(2009).
8) Y. Ding, Y. Wang, and J. Ni, Appl. Phys. Lett. 95, 123105(2009).
9) P.P. Shinde, and V. Kumar, Phys. Rev. B 84, 125401(2011).
10) A.K. Manna, and S.K. Pati, J. Phys. Chem. C 115, 10842 (2011).
11) Q.Peng, and S. De, Physica E44, 1662 (2012).
12) M. Ni, Y. Wang, Q.Yang, Q.Zhu,Q.Tang, and Z. Li, Mod. Phys. Lett. B 28, 1450144 (2014).
13) J. Beheshtian, H. Soleymanabadi, A.A. Peyghan, and Z. Bagheri, Appl. Surf. Sci. 268,436 (2013).
14) M. Kan, J. Zhou, Q. Wang, Q.Sun, and P. Jena, Phys. Rev. B84, 205412 (2011).
15) H. Park, A. Wadehra, J.W. Wilkins, and A.H. Castro Neto, Appl. Phys. Lett. 100, 253115 (2012).
16) Y. Xie, H. Yu, H.X. Zhang, and H.G. Fu, Phys. Chem. Chem. Phys. 14,4391(2012).
17) A. Ramasubramaniam, and D. Naveh, Phys. Rev. B84, 075405 (2011).
18) M.G.Menezes, and R.B. Capaz, Phys. Rev. B86, 195413 (2012).
19) B. Muchharla, A. Pathak, Z. Liu, L. Song, T. Jayasekera, S. Kar, R. Vajtai,L. Balicas, P.M. Ajayan, and S. Talapatra, Nano Lett. 13, 3476 (2013).
20) W.Xie, T. Yanase, T. Nagahama, and T.Shimada, C - J. Carbon Research 2,2 (2016).
21) M. Terrones, N. Grobert, and H. Terrones, Carbon 40, 1665 (2002).

22) A. Vinu, T. Mori, and K. Ariga, Sci. Tech. Adv. Mater. 7, 753 (2006).
23) R.Z. Ma, D. Goldberg, Y. Bando, and T. Sasaki, Phil.Trans. Roy. Soc. London Ser. A 361, 2161 (2004).
24) A.M.Alexander, and J.S.J. Hargreaves, Chem. Soc. Rev. 39, 4388 (2010).
25) T.Tamura, T. Yanase, T. Nagahama, M. Wakeshima, Y. Hinatsu, and T.Shimada, Chem.Lett. 43, 1569 (2014).
26) W. Xie, T. Tamura, T. Yanase, T. Nagahama, and T. Shimada, Ext. Abs. of SSDM2017, B-3-04 (2017).
27) P. Giannozzi, S. Baroni, N. Bonini, M. Calandra, R. Car, C. Cavazzoni, D. Ceresoli, G.L Chiarotti, M.Cococcioni, and I. Dabo, J. Phys. 21, 395502 (2009)
28) G. Kresse, and J. Furthmuller, Phys.Rev.B 54 11169(1996).
29) Q.B.Wang, C.Zhou, J. Wu, T.Lu, and K.H.Je, Comput. Mater. Sci. 102, 196 (2015).
30) M. Etienne, A. Quach, D. Grosso, L. Nicole, C. Sanchez, and A. Walcarius, Chem. Mater. 19, 844 (2007).
31) H.J. Monkhorst and J.D. Pack, Phys. Rev. B13, 5188 (1976).
32) A. D. Becke and K. E. Edgecombe, J. Chem. Phys. 92, 5397 (1990).
33) A. Savin, O. Jepsen, J. Flad, O.K. Andersen, H. Preuss and H.G. von Schnering, Angew. Chem. Int. Ed. 31, 187 (1992).
34) H. Murakami, Bull.Chem.Soc. Jpn. 28, 577 (1955).
35) L. Filipozzi, A. Derre, J. Conard, L. Piraux, and A. Marchand, Carbon 33, 1747 (1995).
36) L. Filipozzi, L. Piraux, A. Marchand, A. Derre, A. Adouard, and M. Kinany-Alaoui, J. Mater. Res. 12, 1711(1997).
37) A. Prakash, and K.B. Sundaram, ECS J. Solid State Sci. & Technol. 4, N25 (2015).
38) T. Tamura, T. Takami, T. Yanase, T. Nagahama, and T. Shimada, Jpn. J. Appl. Phys. 56, 06HF01 (2017).
39) T. Tamura, T. Takami, S. Kobayashi, T. Nagahama, T. Yanase, and T. Shimada, Diamond and Related Materials 69,127 (2016).
40) W. Xie, A. Kawahito, T. Miura, T. Endo, Y. Wang, T. Yanase, T. Nagahama, Y. Otani, and T. Shimada, Chem. Lett. 44 , 1205 (2015).
41) T. Tamura, T. Yanase, T. Nagahama, M. Wakeshima, Y. Hinatsu, and T. Shimada, Chem. Lett. 43, 1569(2014).

Figure Captions

Fig. 1. (Color Online) Typical examples of odd number substitutions. (a) A carbon atom replaces a boron atom. (b) A carbon atom replaces a nitrogen atom. (c) Three carbon atoms replace three boron atoms. (d) Three carbon atoms replace three nitrogen atoms. (e) Three carbon atoms replace a boron atom and two nitrogen atoms. (f) Three carbon atoms replace two boron atoms and a nitrogen atom.

Fig. 2. (Color Online) The electronic band structures of the hypothetical materials. Figures 2(a) - 2(f) correspond to Figs. 1(a) - 1(f), respectively.

Fig. 3. (Color Online) 2D-electron localization function (ELF) distribution of the monolayer h-CBN structures. (a)-(f) correspond to those in Figs.1 and 2 as shown in the insets.

Fig. 4. (Color Online) The optimized structures of the double-layered h-CBN structures. (a) “2C-i”, (b) “2C-ii”, (c) “2C-iii”, (d) “6C-i”, and (e) “6C-ii”. See main text for the naming rule.

Fig. 5. (Color Online) Band structures of the double-layered h-CBN structures. (a)-(e) correspond to those of Fig.4.

Fig. 6. (Color Online) HOMO and LUMO of the double-layered structures. (a) HOMO and (b)LUMO of “2C-i”. (c) HOMO and (d) LUMO of “2C-ii”. (e) HOMO and (f) LUMO of “2C-iii”.

Fig. 7. (Color Online) The ELF of “2C-i”. The two doped carbon atoms shifted from their layers and get close. The ELF cloud can be observed between these two doping carbon along the C-C direction which means the C-C bonds formed and it is the σ-bonds.

Fig. 8. (Color Online) The ELF distribution of “2C-ii”.

Fig. 9. (Color Online) The ELF distribution of “6C-ii”. In the bottom layer, the doping three carbon gathered more electron than the top layer.

Fig. 10. (Color Online) The ELF distribution of “2C-iii”

Table 1: Bandgaps and nearest interlayer distances of the unevenly substituted double layer h-BNs

Structure	"2C-i"	"6C-i"	"2C-ii"	"6C-ii"	"2C-iii"
Bandgap (eV)	3.75	3.25	0.36	0.61	2.69
Nearest Interlayer (Å) Distance	1.67	1.67	2.71	2.70	1.76

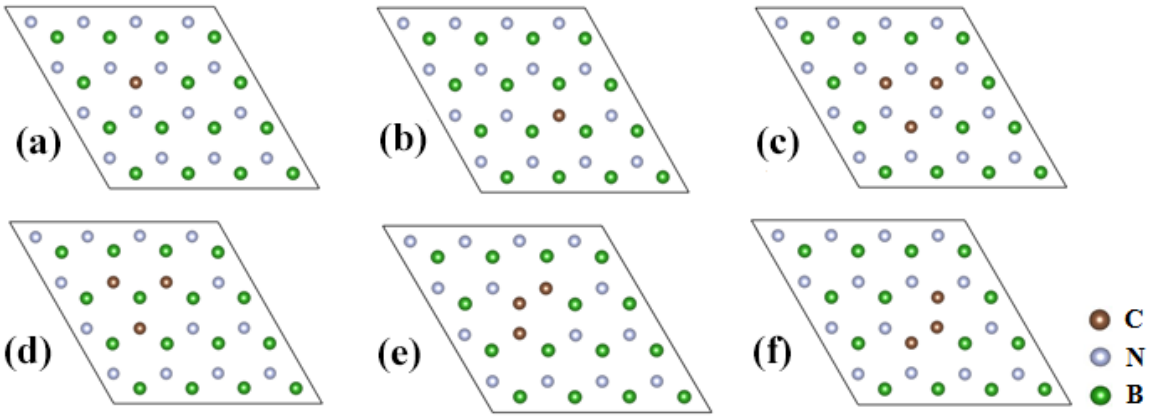

Fig. 1. (Color Online) Typical examples of odd number substitutions. (a) A carbon atom replaces a boron atom. (b) A carbon atom replaces a nitrogen atom. (c) Three carbon atoms replace three boron atoms. (d) Three carbon atoms replace three nitrogen atoms. (e) Three carbon atoms replace a boron atom and two nitrogen atoms. (f) Three carbon atoms replace two boron atoms and a nitrogen atom.

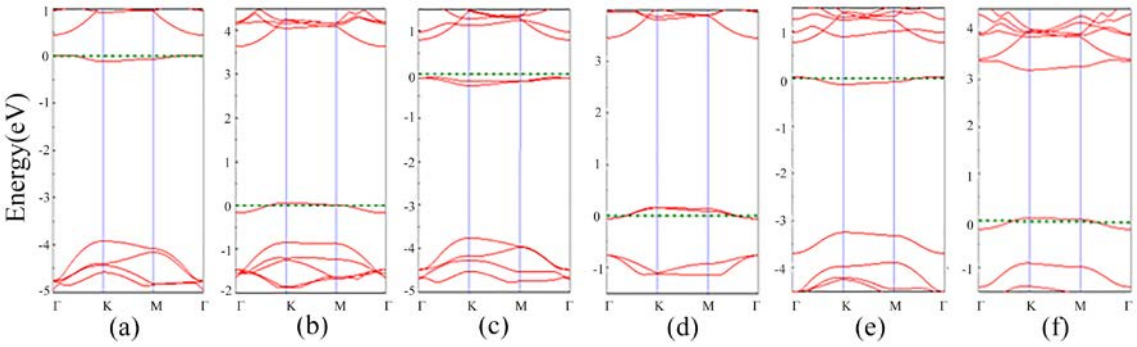

Fig. 2. (Color Online) The electronic band structures of the hypothetical materials. Figures 2(a) - 2(f) correspond to Figs. 1(a) - 1(f), respectively.

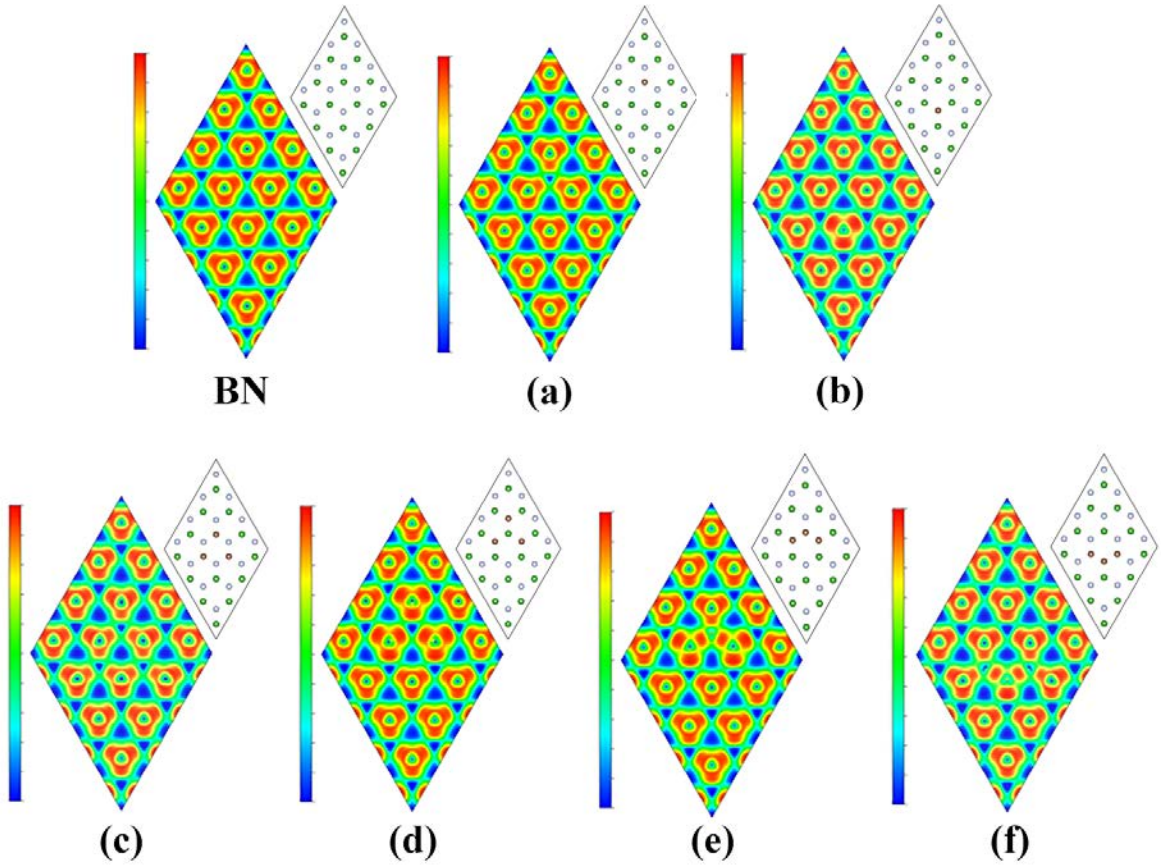

Fig. 3. (Color Online) 2D-electron localization function (ELF) distribution of the monolayer h-CBN structures. (a)~(f) correspond to those in Figs.1 and 2 as shown in the insets.

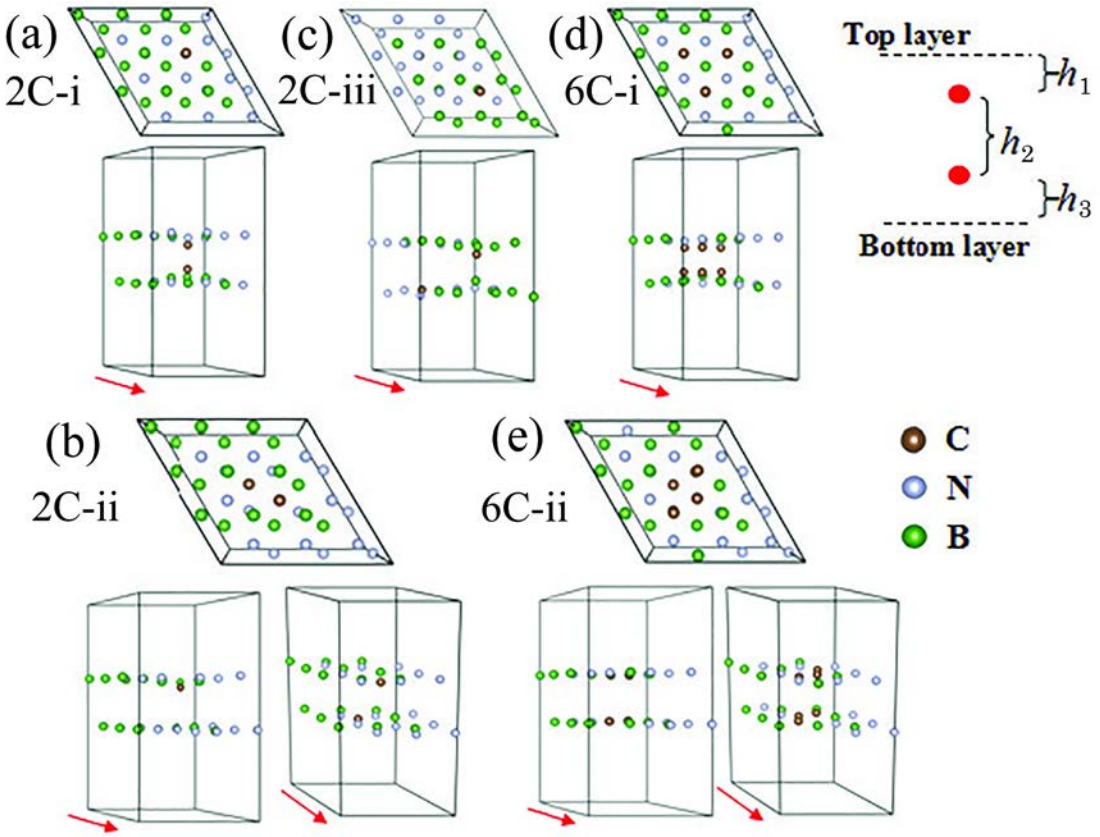

Fig. 4. (Color Online) The optimized structures of the double-layered h-CBN structures. (a) "2C-i", (b) "2C-ii", (c) "2C-iii", (d) "6C-i", and (e) 6C-ii. See main text for the naming rule.

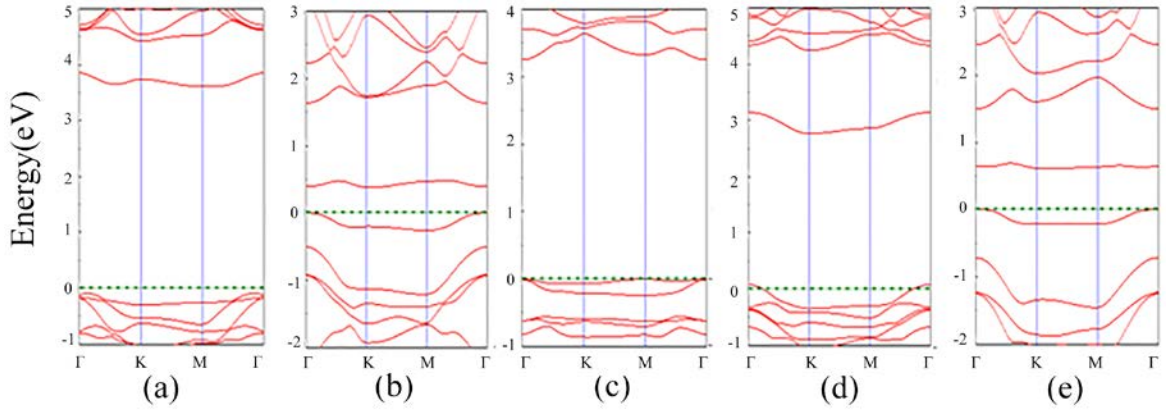

Fig. 5. (Color Online) Band structures of the double-layered h-CBN structures. (a)-(e) correspond to those of Fig.4.

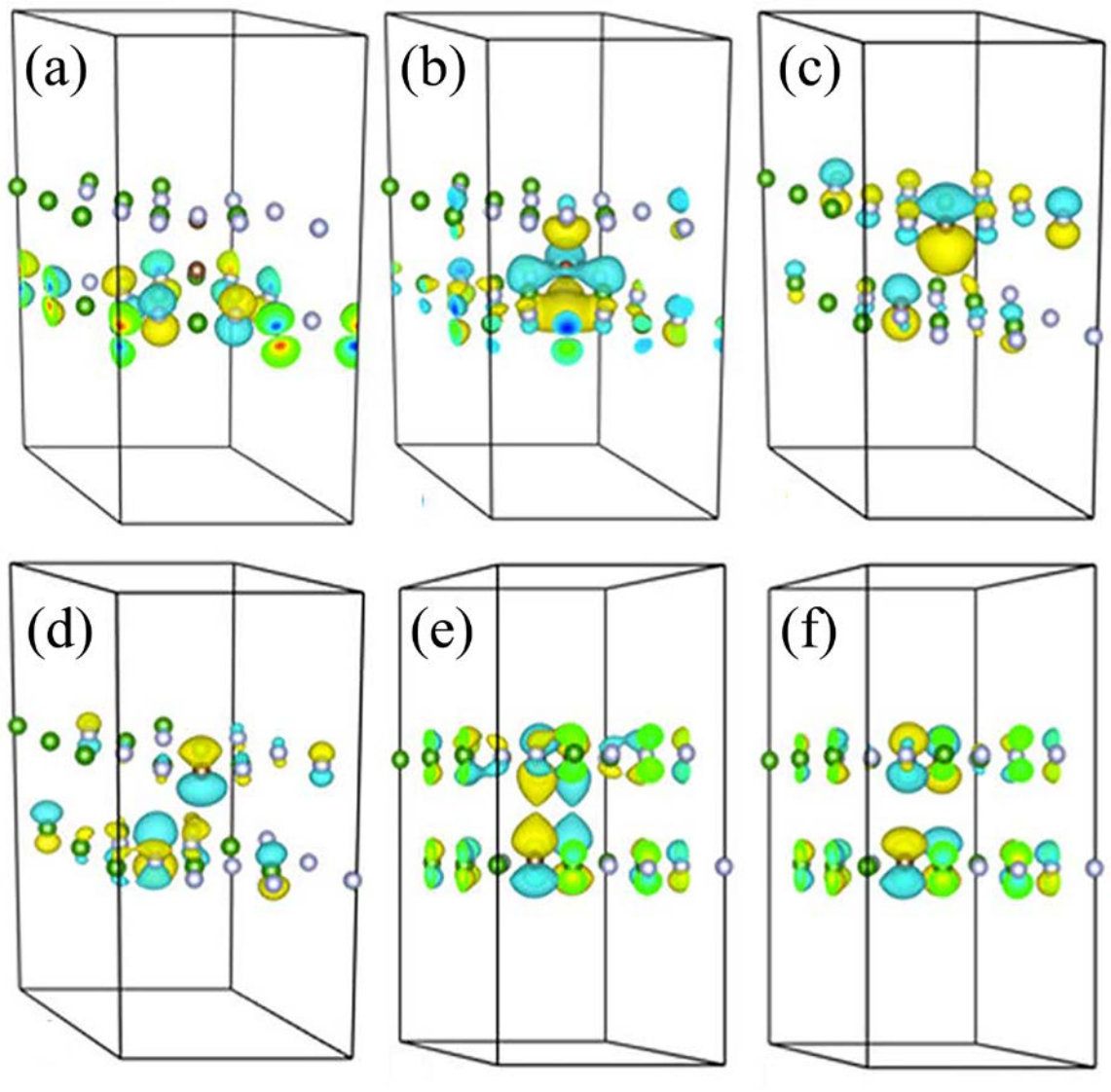

Fig. 6. (Color Online) HOMO and LUMO of the double-layered structures.

(a) HOMO and (b)LUMO of “2C-i”. (c) HOMO and (d) LUMO of “2C-ii”. (e) HOMO and (f) LUMO of “2C-iii”.

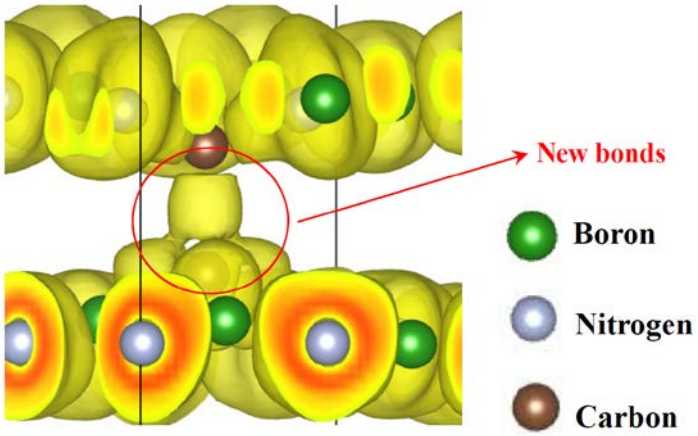

Fig. 7. (Color Online) The ELF distrubution of “2C-i”. The two doped carbon atoms shifted from their layers and get close. The ELF cloud can be observed between these two doping carbon along the C-C direction which means the C-C bonds formed and it is the σ-bonds.

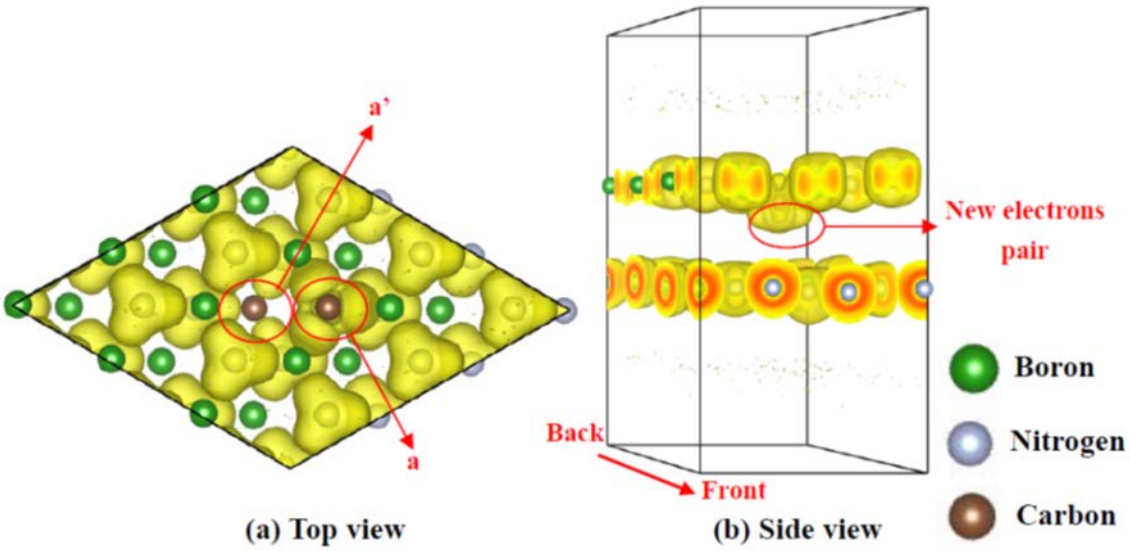

Fig. 8. The ELF distribution of “2C - ii”.

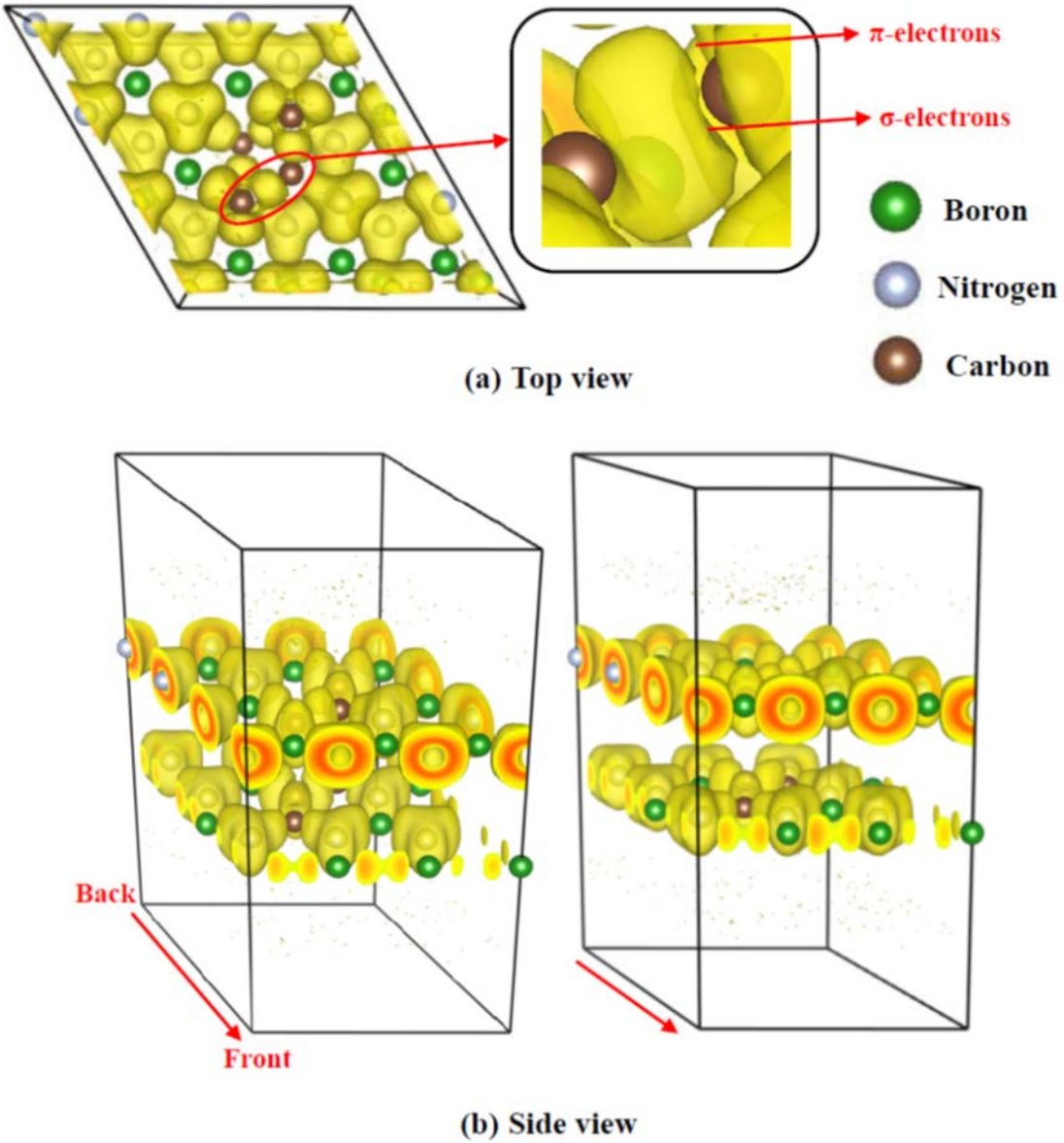

Fig. 9. The ELF distribution of "6C-ii". In the bottom layer, the doping three carbon gathered more electron than the top layer.

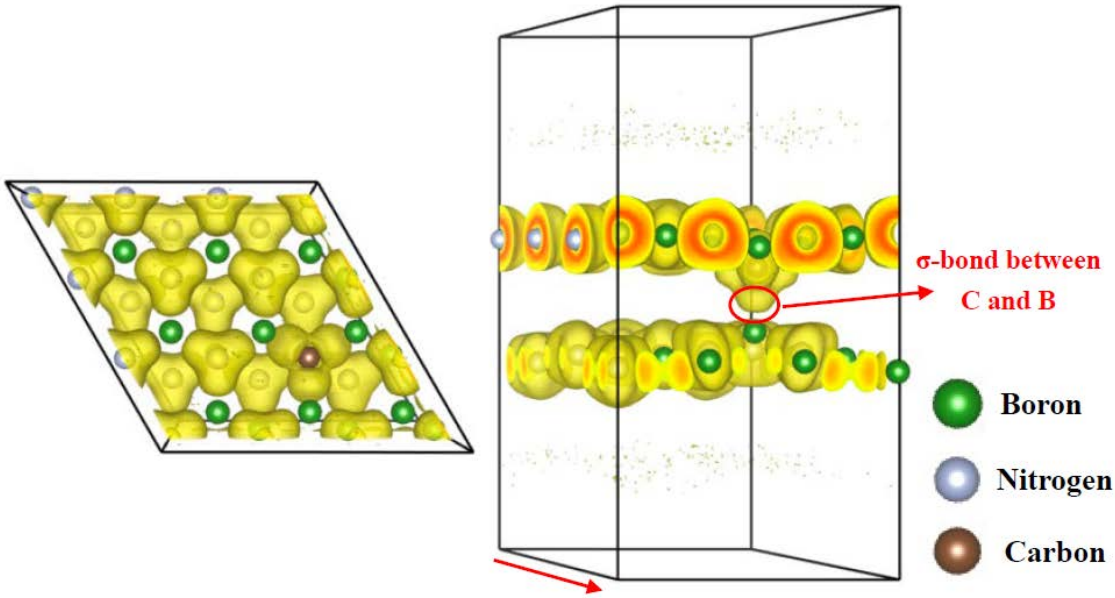

Fig. 10. The ELF distribution of “2C - iii”.